Cite as: L. F. Mager *et al.*, *Science* 10.1126/science.abc3421 (2020).

Microbiome-derived inosine modulates response to checkpoint inhibitor immunotherapy

Lukas F. Mager[1]*, Regula Burkhard[2], Nicola Pett[1], Noah C. A. Cooke[1], Kirsty Brown[1], Hena Ramay[3], Seungil Paik[4], John Stagg[5], Ryan A. Groves[6], Marco Gallo[4], Ian A. Lewis[6], Markus B. Geuking[2], Kathy D. McCoy[1]*

[1]Department of Physiology and Pharmacology, Snyder Institute of Chronic Diseases, Cumming School of Medicine, University of Calgary, Calgary, Canada. [2]Department of Microbiology, Immunology and Infectious Diseases, Snyder Institute of Chronic Diseases, Cumming School of Medicine, University of Calgary, Calgary, Canada. [3]International Microbiome Centre, Cumming School of Medicine, University of Calgary, Calgary, Canada. [4]Department of Biochemistry and Molecular Biology and Department of Physiology and Pharmacology, Charbonneau Cancer Institute, Alberta Children's Hospital Research Institute, Cumming School of Medicine, University of Calgary, Calgary, Canada. [5]Centre de Recherche du Centre Hospitalier de l'Université de Montréal et Institut du Cancer de Montréal, Québec, Canada. [6]Department of Biological Sciences, University of Calgary, Calgary, Canada.

*Corresponding author. Email: kathy.mccoy@ucalgary.ca (K.D.M.); lukas.mager@ucalgary.ca (L.F.M.)

Several species of intestinal bacteria have been associated with enhanced efficacy of checkpoint blockade immunotherapy, but the underlying mechanisms by which the microbiome enhances anti-tumor immunity is unclear. Here, we isolated three bacterial species, including *Bifidobacterium pseudolongum*, *Lactobacillus johnsonii* and *Olsenella* species, that significantly enhanced efficacy of immune checkpoint inhibitors in four mouse models of cancer. We found that intestinal *B. pseudolongum* modulated enhanced immunotherapy response through production of the metabolite inosine. Decreased gut barrier function induced by immunotherapy increased systemic translocation of inosine and activated anti-tumor T cells. The effect of inosine was dependent on T cell expression of the adenosine A_{2A} receptor and required co-stimulation. Collectively, our study identifies a novel microbial metabolite-immune pathway that is activated by immunotherapy that may be exploited to develop microbial-based adjuvant therapies.

Immune checkpoint blockade (ICB) therapy can be an effective therapy in some tumors and certain cancer patients by harnessing the therapeutic potential of the immune system. Targeting cytotoxic T-lymphocyte-associated antigen 4 (CTLA-4), programmed cell death protein 1 (PD-1) or its ligand (PD-L1) has revolutionized the treatment of some cancers, including melanoma, renal cell carcinoma, and non-small cell lung cancer (*1*, *2*). Nevertheless, many other cancers show primary resistance to ICB therapy and response rates remain low and differ between patients even in those cancers where ICB therapy has provided benefit (*3*–*5*). There is therefore an urgent need to determine the underlying reasons for such non-responsiveness. Recent studies have provided strong evidence that the gut microbiota can affect anti-tumor immunity, and composition of the intestinal microbiome may even predict the efficacy of ICB therapy. A series of seminal studies revealed that the efficacy of ICB therapies was dependent on specific gut bacteria (*6*–*10*) and treatment with ICB-promoting bacteria may help to overcome primary resistance to ICB therapies (*8*). Despite the findings that specific bacterial species have been associated with increased anti-tumor immunity, the precise molecular mechanisms by which these microbes enhance ICB therapy remain elusive. In this study, we utilized an animal model of colorectal cancer (CRC) to identify specific ICB-promoting bacteria, elucidated the underlying molecular mechanism of how these microbes enhanced ICB therapy efficacy and validated our findings in additional models of bladder cancer and melanoma.

Although the intestinal microbiota can affect CRC progression (*11*, *12*) and may alter the efficacy of chemotherapeutics (*13*, *14*), clinically, ICB therapies are notoriously ineffective in most CRC cases (*15*) and the role of the microbiome in non-responsiveness has not yet been determined. We therefore investigated the efficacy of ICB therapy in a mouse model where colonic tumors are induced using azoxymethane (AOM) and dextran sulfate sodium (DSS) (Fig. 1A). Notably, treatment with anti-CTLA-4 or anti-PD-L1 antibodies led to significantly fewer and smaller tumors (Fig. 1, B and C) and reduced the frequency of $EpCam^+Lgr5^+$ cells in the tumor, markers for epithelial cell stemness (Fig. 1D). Anti-CTLA-4 treatment also resulted in increased immune cell infiltration into the tumors (Fig. 1E). Increased $CD8^+$ T cell frequencies in the tumor draining lymph node (fig. S1A) was also observed together with increased $IFN\gamma^+CD4^+$ and $IFN\gamma^+CD8^+$ T cells in the spleen (fig. S1, B and C). In this model, the effects of anti-CTLA-4 were greater than those induced by anti-PD-L1 treatment when using the same antibody dose. The difference in anti-CTLA-4 and anti-PD-L1 efficacy in this model may be dependent on dose-effect relationship and higher doses have previously been described for anti-PD1 therapy (*8*). Moreover, effector functions of anti-

CTLA-4 and anti-PD1/PD-L1 rely on distinct mechanisms, among them regulatory T cells (*16*) and indeed Treg composition and function are different between cancer types, also in intestinal tumors (*17*). We next used this model system to screen for potentially beneficial bacteria that were associated with ICB responsiveness. Although no significant changes were observed in the overall fecal bacterial composition (β-diversity) between ICB-treated and control mice (fig. S1D), a few bacterial families were differentially abundant (fig. S1E). In contrast, sequencing of tumor-associated bacterial communities revealed differences in β-diversity (fig. S1F) and additional bacterial genera were differentially abundant in the ICB-treated tumors (Fig. 1F and fig. S1, G and H). We therefore performed anaerobic culture of homogenized tumors from both groups and were able to culture and identify twenty-one distinct bacterial isolates. Seven bacterial species were cultured only from ICB-treated tumors, whereas four were found only in the control group (Fig. 1G). Of note, *Bifidobacterium pseudolongum* was one of the isolates cultured only from ICB-treated tumors. *B. pseudolongum* belongs to the genus *Bifidobacterium*, which was identified as differentially abundant by sequencing (Fig. 1F and fig. S1, G and H). Interestingly, *Akkermansia muciniphila*, which was recently identified to enhance the efficacy of anti-PD-L1 and anti-PD-1 treatments in lung and kidney cancers (*8*), was also one of the seven bacteria cultured only from ICB-treated tumors (Fig. 1G). Isolation and identification of distinct bacterial species associated with ICB responsiveness provided us with the opportunity to identify the molecular mechanism involved.

Next, we determined whether the efficacy of ICB therapy in CRC was dependent on the microbiota, as has been shown with other tumor types (*6*). As the development of orthotopic adenocarcinomas is severely reduced in animals with a limited microbiota (*18*), we switched to a heterotopic in vivo model of CRC where MC38 colorectal cancer cells were implanted into the flank of germ-free (GF) or specific pathogen-free (SPF) mice followed by ICB therapy once tumors were palpable (fig. S2A). Anti-CTLA-4 treatment led to smaller tumors (fig. S2B) and markedly increased intratumoral and splenic $CD4^+$ and $CD8^+$ T cell activation and proliferation in SPF compared to GF mice (fig. S2, C to F). To ensure the lack of ICB efficacy was not merely a reflection of the immature immune system of GF mice, we also assessed the effect of ICB therapy in antibiotic-treated SPF mice (fig. S2G). Similar to GF mice, broad spectrum antibiotics also reduced ICB therapy efficacy in tumor-bearing SPF mice (fig. S2, H to J).

To evaluate whether the isolated bacteria that were enriched in the tumors of ICB-treated mice (Fig. 1G) were able to boost the efficacy of ICB therapy, GF mice were monocolonized with five different isolated bacterial species. MC38 tumor cells were injected heterotopically into monocolonized or GF mice and, upon palpable tumor development, all mice were treated with anti-CTLA-4 and tumor growth and anti-tumor immunity assessed (Fig. 1H). Of the five bacteria tested, monocolonization with *B. pseudolongum*, *Lactobacillus johnsonii* (*L. johnsonii*) and *Olsenella* species significantly enhanced the efficacy of anti-CTLA-4 treatment compared to GF mice or mice monocolonized with *Colidextribacter* species or *Prevotella* species (Fig. 1, I and J, and fig. S3, A and B). In addition, $CD4^+$ and $CD8^+$ T cell activation was substantially increased (Fig. 1K) whereas proliferation of intratumoral $CD8^+$ T cells (fig. S3, C and D) was modestly increased in the tumors of *B. pseudolongum*, *L. johnsonii* and *Olsenella* species monocolonized animals. The isolated ICB-promoting *B. pseudolongum* strain also improved the efficacy of anti-PD-L1 treatment in the MC38 heterotopic tumor model compared to the *Colidextribacter* species control bacteria (fig. S4), albeit to a lower extent than observed for anti-CTLA-4 treatment (at the same dose), similar to our observations in the AOM/DSS model. Since *B. pseudolongum* provided the most robust ICB-promoting effect, it was selected for further mechanistic studies. Of note, other *Bifidobacterium* species, such as *B. breve* and *B. longum*, have previously been found to promote antitumor immunity and enhance anti-PD-L1 efficacy in a murine model of melanoma (*7*). In humans, *B. longum* has been reported to be enriched in anti-PD1 responders (*9*). Furthermore, *B. pseudolongum* species are widely distributed in the mammalian gut with many different strains displaying genomic diversity and differential metabolic capacities (*19*), suggesting strain-dependent functions.

We found that anti-tumor immunity was dependent on ICB therapy as monocolonization with *B. pseudolongum* in the absence of anti-CTLA-4 treatment was not able to reduce tumor growth (fig. S5, A to C) or induce anti-tumor immunity (fig. S5, D and E), which is similar to previous studies with other ICB-promoting bacteria (*6*, *8*). Importantly, while previous studies have shown that some bacteria accumulate in the tumor environment where they locally stimulate the immune system and kill tumor cells through toxic metabolites (*20*), we could not detect *B. pseudolongum* within the heterotopic tumors (fig. S6). Therefore, despite the fact that *B. pseudolongum* was initially isolated from intestinal tumors, the presence of bacteria within tumors was not required for the enhancement of ICB therapy in our model, suggesting the potential involvement of soluble factors.

Although *B. pseudolongum* did not induce anti-tumor immunity in the absence of ICB therapy (fig. S5), intestinal *B. pseudolongum* induced a significant increase in expression of the Th1 master transcription regulator T-bet in small intestinal lamina propria $CD4^+$ T cells, which was not observed in GF or *Colidextribacter* species-monocolonized mice (Fig. 2, A and B). This illustrated that *B. pseudolongum* has immunomodulatory capacity even in the absence of ICB. In the

absence of ICB, this effect was restricted to the gut-associated lymphoid tissue (GALT) as it was also observed, albeit to a lower extent, in the mesenteric lymph nodes (MLN) (fig. S7A), but not in the spleen (Fig. 2C). In the absence of ICB, *B. pseudolongum* did not increase the activation of effector function of Th1 cells as IFN-γ^{+}T-bet^{+} cells did not differ from controls in any of the tissues assessed (Fig. 2, B and C, and fig. S7A). Taken together, in the absence of tumors and ICB therapy, *B. pseudolongum* promoted mucosal Th1 transcriptional differentiation in GALT without increasing effector function in the gut and draining lymph nodes. While *B. pseudolongum* had no effect on other CD4^{+} T cell subsets in the small intestine (fig. S7B), it did increase CD8^{+}T-bet^{+} T cells (fig. S7C). Moreover, *B. pseudolongum* had minimal impact on Th17 and regulatory T (Treg) cells in the MLN and spleen (fig. S7, D to G).

Since *B. pseudolongum* monocolonization in the absence of tumors and ICB therapy induced only local mucosal Th1 differentiation during homeostasis, we next asked whether the combination of *B. pseudolongum* and anti-CTLA-4 therapy (in the absence of a tumor) would lead to systemic Th1 activation. Indeed, colonization with *B. pseudolongum* combined with ICB treatment led to significantly enhanced splenic Th1 cell activation and effector function as evidenced by IFN-γ production compared to *Colidextribacter* species-monocolonized or GF animals (Fig. 2, D and E, and fig. S7, H and I). We concluded that *B. pseudolongum* induces Th1 differentiation and, together with anti-CTLA-4, activation of Th1 effector T cells. Interestingly, a recently defined consortium of eleven bacteria (that did not include any *Bifidobacterium spp.*) induced IFN-γ production preferentially in CD8^{+} T cells and promoted anti-tumor immunity in the absence of immunotherapy (*21*). In contrast, *B. pseudolongum* induced IFN-γ production in both CD4^{+} and CD8^{+} T cells (fig. S7J), and ICB treatment was required for anti-tumor immunity.

We were intrigued by the ability of *B. pseudolongum* to induce Th1 transcriptional differentiation during homeostasis versus activation of Th1 effector function following ICB treatment. Gastrointestinal inflammation is a common immune-related adverse effect of anti-CTLA-4 treatment (*1*) and we reasoned that this may be due to alterations in gut barrier integrity. Indeed, monocolonized animals treated with anti-CTLA-4 displayed increased systemic serum anti-commensal antibody reactivity, particularly Th1-associated IgG2b, and reduced small intestinal transepithelial electrical resistance compared to controls (fig. S8, A and B). Despite this, anti-CTLA-4 treatment did not induce overt local or systemic inflammation (fig. S8, C and D). In this regard, it is interesting that some *Bifidobacterium* species have been reported to provide protection from anti-CTLA-4-induced enterocolitis with no effect on tumor growth (*22*). The induction of systemic anti-bacterial antibodies following ICB therapy was not required for the ICB-promoting effect as anti-CTLA-4 treatment was also effective in *B. pseudolongum* monocolonized mice deficient in B cells and antibodies (fig. S9). Therefore, since bacteria did not accumulate in (heterotopic) tumors (fig. S6), anti-CTLA-4 reduced the integrity of the gut barrier (fig. S8), and B cells and anti-commensal antibodies were not required for the ICB-promoting effect of *B. pseudolongum* (fig. S9), we hypothesized that increased systemic translocation of metabolites may be responsible for the systemic effect of *B. pseudolongum* during ICB therapy. To address this, serum collected from tumor-bearing GF, *B. pseudolongum* or *Colidextribacter* species-monocolonized mice treated with anti-CTLA-4 was transferred concomitantly with anti-CTLA-4 into GF MC38 tumor-bearing mice (Fig. 2F). Remarkably, serum from anti-CTLA-4-treated *B. pseudolongum* monocolonized mice, but not from anti-CTLA-4-treated GF or *Colidextribacter* species-monocolonized mice, was sufficient to reduce tumor growth and elicit strong anti-tumor immunity in the tumor and spleen of GF mice (Fig. 2, G to I, and fig. S10). In summary, these data show that soluble factors derived from—or induced by—*B. pseudolongum* were responsible for the observed ICB-promoting effects.

Untargeted metabolomics of the serum samples revealed increased levels of several metabolites in sera from *B. pseudolongum* compared to *C.* sp. monocolonized and GF mice (Fig. 2J and fig. S11, A and B). Notably, the purine metabolite inosine was the only metabolite that was significantly more abundant (8 to 9-fold) in sera from *B. pseudolongum* monocolonized mice compared to sera from *Colidextribacter* species-monocolonized or GF mice (Fig. 2K). Of note, xanthine and hypoxanthine, degradation products of inosine, were also elevated in the sera of *B. pseudolongum* monocolonized mice (table S1). Analysis of bacterial culture supernatant revealed that both *B. pseudolongum* and *A. muciniphila* produced significantly higher amounts of inosine than *Colidextribacter* species. under the same culture conditions (fig. S11C), revealing that inosine is a bacterial metabolite produced by *B. pseudolongum* and *A. muciniphila.* In contrast, while *L. johnsonii* did not produce inosine, it did produce high amounts of hypoxanthine compared to *Colidextribacter* species (fig. S11D), a potent ligand binding to the same receptor as inosine (*23*). Of note, inosine monophosphate and hypoxanthine were two of the most elevated metabolites in the cecum and serum of mice colonized with the consortium of eleven bacteria that Tanoue *et al.* recently identified to improve ICB therapies (*21*). The identity of inosine was confirmed by fragmentation analysis (fig. S11E).

To determine the physiological inosine levels in vivo we measured inosine concentrations in duodenal, jejunal and cecal contents of *B. pseudolongum* monocolonized mice. Inosine concentrations were highest in the duodenum and gradually decreased along the gastrointestinal tract

(duodenum 66.13 ±14.23 μM > jejunum 29.26 ± 9.38 μM > cecum 0.5 ± 0.05 μM; fig. S11F). We also quantified inosine concentrations in the serum of anti-CTLA-4- and anti-PD-L1-treated *B. pseudolongum* (anti-CTLA-4: 26.16 ± 3.32 μM, anti-PD-L1: 37.5 ± 10.2 μM) and *Colidextribacter* species. (anti-CTLA-4: 3.26 ±1.01 μM, anti-PD-L1: 4.8 ± 1.3 μM) monocolonized mice (fig. S11F), in the serum of SPF mice before (4.08 ± 1.12 μM) and after anti-CTLA-4 treatment (11.65 ± 2.09 μM), and in the serum of antibiotic-treated SPF mice given anti-CTLA-4 (2.03 ± 0.86 μM; fig. S11G). These data indicated that bacterial production of inosine in the upper gastrointestinal tract is likely to be the predominant source of elevated systemic inosine levels in *B. pseudolongum* monocolonized mice.

The identification of inosine was initially surprising because inosine binds to the adenosine 2A receptor ($A_{2A}R$), which has been demonstrated to have an inhibitory effect of inosine on Th1 differentiation in vitro and anti-tumor immunity in vivo (*24–27*). Indeed, data supporting an immunosuppressive role for adenosine and $A_{2A}R$ signaling has led to the development of novel immune checkpoint inhibitor targets, such as mAb targeting CD73, CD39 and CD38, and pharmacological antagonists of $A_{2A}R$, many of which are currently in clinical trials [reviewed in (*28*)]. However, a small body of literature has demonstrated that inosine analogs can be pro-inflammatory and $A_{2A}R$ signaling can sustain Th1/anti-tumor immunity in mice (*29–31*). Based on these opposing findings, we investigated whether inosine could enhance Th1 cell differentiation in vitro. Activated $OVA_{323-339}$ peptide-pulsed bone marrow derived dendritic cells (BMDCs) were co-cultured with naïve $OVA_{323-339}$-specific OT-II $CD4^+$ T cells in the presence or absence of inosine. Intriguingly, the effect of inosine in terms of induction or inhibition of $CD4^+$ Th1 T cell differentiation turned out to be context dependent. Specifically, in the presence of exogenous IFN-γ, inosine strongly boosted Th1 differentiation of naïve T cells (Fig. 3A), whereas in the absence of IFN-γ, inosine inhibited Th1 differentiation (Fig. 3B and fig. S12A). We next dissected the molecular mechanism through which inosine enhanced Th1 differentiation. While pharmacological inhibition of $A_{2A}R$ signaling (ZM241385) completely abrogated the effect of inosine, addition of cell permeable cyclic AMP (db-cAMP), a signaling molecule downstream of $A_{2A}R$, restored Th1 differentiation and bypassed the need for inosine (Fig. 3A). Furthermore, inhibition of protein kinase A (PKA), a downstream effector molecule of cAMP, negated inosine driven Th1 differentiation (Fig. 3A). In addition, the inosine-$A_{2A}R$-cAMP-PKA signaling cascade led to phosphorylation of the transcription factor cAMP response element-binding protein (CREB; fig. S12B), a known transcriptional enhancer of key Th1 differentiation factors, such as IL-12 receptor and IFN-γ (*32–34*). Indeed, we also observed inosine-dependent up-regulation of IL12Rβ2 (fig. S12C).

The effect of inosine was T cell-intrinsic because the addition of inosine to naïve T cells that had been activated with anti-CD3/anti-CD28-coated beads also enhanced Th1 differentiation, even in the absence of IFN-γ (fig. S12D). In addition, induction of Th1 differentiation and phosphorylation of CREB was absent when $A_{2A}R$-deficient T cells were stimulated with inosine (fig. S12, E and F). In contrast, bypassing the need for $A_{2A}R$ signaling by using db-cAMP increased Th1 differentiation and phosphorylation of CREB in $A_{2A}R$-deficient T cells, confirming that the Th1 promoting effect of inosine is dependent on $A_{2A}R$ signaling (fig. S12, E and F). In addition, since pCREB is known to bind to key Th1 target genes, we also confirmed that inosine stimulation led to a sustained up-regulation of *Il12rb2* and *Ifng* gene expression in $CD4^+$ T cells (fig. S12, G and H). Importantly, inosine dose response experiments revealed that the physiological concentrations of inosine observed in sera of *B. pseudolongum* but not *Colidextribacter* species monocolonized mice were sufficient to induce Th1 activation (fig. S12I). In contrast, adenosine, which also binds to the $A_{2A}R$, was present only at extremely low levels in intestinal contents, and serum levels did not differ between *B. pseudolongum* and *Colidextribacter* species monocolonized mice (fig. S12J), indicating that adenosine was unlikely to be mediating the ICB-promoting effects of *B. pseudolongum*. Furthermore, adenosine dose-response experiments revealed that the levels of adenosine in the serum were insufficient to promote Th1 activation and effector function (fig. S12K). To confirm whether the inosine mediated Th1 promoting effect in vitro also applied to in vivo conditions, GF mice were immunized with ovalbumin in combination with CpG as a co-stimulus. Of note, we utilized CpG as a co-stimulus as it is a widely used anti-tumor adjuvant in different settings [reviewed in (*35*)]. One day later, mice received inosine or vehicle by intraperitoneal administration. Inosine increased the proportions of $T\text{-bet}^+IFN\text{-}\gamma^+CD8^+$ and $T\text{-bet}^+IFN\text{-}\gamma^+CD4^+$ T cells in the MLN (fig. S12, L to N), validating our in vitro results.

We next determined whether the ICB-enhancing ability of *B. pseudolongum* required $A_{2A}R$ expression specifically on T cells. Anti-tumor immunity was assessed in *B. pseudolongum* monocolonized *Rag1*-deficient mice bearing MC38 tumors that had been adoptively transferred with either $A_{2A}R$-deficient or wild-type T cells and treated with anti-CTLA-4 (Fig. 3C). We found that the absence of $A_{2A}R$ expression on T cells reduced the ICB-promoting effect of *B. pseudolongum* (Fig. 3, D and E).

We then determined whether inosine could promote anti-tumor immunity induced by anti-CTLA-4 in the absence of *B. pseudolongum*. GF mice were challenged with MC38 tumor cells and upon palpable tumors, inosine or PBS was given orally or systemically in combination with anti-CTLA-4 treatment and CpG as a co-stimulus (Fig. 3F). Compared to PBS,

both oral and systemic administration of inosine led to reduced tumor weights and increased anti-tumor immunity when given together with anti-CTLA-4 and CpG (Fig. 3, G and H). In contrast, in the absence of CpG, inosine increased tumor weights and reduced anti-tumor immunity (Fig. 3, G and H), validating our previous in vitro findings demonstrating that the effect of inosine was context-dependent and based on the presence or absence of co-stimulation. Inosine-induced anti-tumor immunity was also dependent on $A_{2A}R$ signaling in T cells as oral supplementation with inosine failed to induce anti-tumor immunity in MC38 tumor-bearing germ-free *Rag1*-deficient animals adoptively transferred with $A_{2A}R$-deficient T cells (Fig. 3, I to K). These data indicated that the ICB-promoting effect of *B. pseudolongum* was mediated by inosine and was dependent on $A_{2A}R$ signaling specifically in T cells.

Since we detected *A. muciniphila* in ICB-treated tumors (Fig. 1G), and was previously shown to increase ICB therapy efficacy (*8*) and to produce inosine in vitro (fig. S11C), we further investigated whether *A. muciniphila* also relies on $A_{2A}R$ signaling to enhance ICB-therapy efficacy. We found that monocolonization with *A. muciniphila* in combination with anti-CTLA-4 led to smaller tumors and increased anti-tumor immunity and this was dependent on T cell expression of $A_{2A}R$ (fig. S13, A to D). Although monocolonization with *L. johnsonii* was able promote the anti-tumor effects of anti-CTLA-4 (Fig. 1, I to K, and fig. S5), hypoxanthine (another ligand of the $A_{2A}R$), and not inosine, was elevated in in vitro cultures (fig. S11, C and D). Despite this, the ICB-promoting effect of *L. johnsonii*, although less potent than that of *B. pseudolongum* and *A. muciniphila*, was also partially dependent on T cell expression of $A_{2A}R$ (fig. S13, E to H).

We next tested whether inosine could also promote the efficacy of anti-CTLA-4 therapy in the presence of a complex microbiota. We first utilized a gnotobiotic model where mice are stably colonized with a defined microbiota consisting of 12 bacterial species, referred to as Oligo-Mouse-Microbiota-12 (Oligo-MM^{12}) (*36*), which lacks *B. pseudolongum*. We found that inosine was able to promote the anti-tumor effects of anti-CTLA-4 with reduced tumor size and increased intratumoral IFN-γ^+CD8$^+$ and IFN-γ^+CD4$^+$ T cells even in gnotobiotic Oligo-MM^{12} mice (fig. S14, A to D). We also found that inosine could promote the efficacy of anti-CTLA-4 in SPF mice, that contain a highly diverse microbiota (fig. S14, E to H). We then examined whether *B. pseudolongum* needed to be viable to enhance anti-CTLA-4 efficacy. While gavage of live *B. pseudolongum*, with or without antibiotic pretreatment, enhanced anti-CTLA-4 effects in SPF mice (fig. S14, E to H), heat-killed *B. pseudolongum* was unable to boost the effects of ICB therapy, likely due to the inability to produce inosine (fig. S14, E to H).

In addition to direct stimulation of T cells, inosine could potentially affect tumor cells directly through altering tumor cell survival or susceptibility to T cell-mediated killing. However, direct in vitro exposure of MC38 tumor cells to inosine did not modulate tumor cell viability (fig. S15A) and pretreatment of MC38 tumor cells prior to co-culture with activated tumor-specific T cells did not promote or inhibit T cell-mediated killing of tumor cells (fig. S15B), further supporting the conclusion that the anti-tumor effect of inosine was mediated primarily through T cells.

Combined, these data indicate that the effect of inosine on T cells required sufficient co-stimulation (likely by DCs), IL-12 receptor engagement for Th1 differentiation and IFN-γ production for efficient anti-tumor immunity. Indeed, conventional dendritic cells (cDCs) were found to be the primary source of IL-12 compared to macrophages (fig. S16, A and B). To further assess the role of cDCs in ICB-bacteria co-therapy, bone marrow (BM) cells from cDC-DTR mice were transferred into lethally γ-irradiated recipient SPF mice to allow for inducible, conditional depletion of cDCs. Following BM reconstitution, mice were treated with antibiotics and gavaged with a mixture of the three previously identified ICB-promoting bacteria, *B. pseudolongum*, *L. johnsonii* and *Olsenella* species. Ten weeks later, mice were implanted with MC38 cells and when palpable tumors were established, cDCs were depleted by injection of diphtheria toxin followed by anti-CTLA-4 treatment (fig. S16C). Depletion of cDCs led to larger tumors (fig. S16D), a significant reduction in intratumoral CD8$^+$ and CD4$^+$ T cell frequencies and IFN-γ production (fig. S16E), and markedly reduced IFN-γ production and proliferation of splenic CD8$^+$ and CD4$^+$ T cells (fig. S16F). Therefore, depletion of cDC strongly reduced the efficacy of the bacteria-elicited ICB response to reduce established tumors, which indicated the requirement for continuous antigen presentation, IL-12 production and T cell co-stimulation by cDCs for efficient ICB therapy. The critical involvement of cDC and IL-12 has previously been reported for anti-PD-1 treatment (*37*).

Since enhanced Th1 immunity is generally considered to be beneficial for most anti-tumor responses [reviewed in (*38*)], we next determined whether intestinal colonization with the isolated ICB-promoting bacteria or treatment with inosine would be equally effective in other tumor models. First, we tested the ICB-promoting effect of *B. pseudolongum*, *L. johnsonii* and *Olsenella* species in SPF *Msh2$^{LoxP/LoxP}$Villin-Cre* (*39*) animals that have conditional inactivation of Msh2 (a DNA mismatch repair gene) in intestinal epithelial cells and develop adenocarcinomas in the small intestine. Previous reports have shown greater efficacy of ICB in mismatch repair deficient (MMRD) cancer in the clinical setting (*15*, *40*). In the *Msh2$^{LoxP/LoxP}$Villin-Cre* model, anti-CTLA-4 treatment alone (without the addition of ICB-promoting bacteria)

led to reduced tumor weights and EpCam^{+}Lgr5^{+} cells in the tumor, markers for epithelial cell stemness, and increased T cell activation and immune cell infiltration in the tumor (fig. S17, A to F). Co-treatment with ICB-promoting bacteria markedly boosted the effect of anti-CTLA-4 (fig. S17G), leading to a further reduction of tumor weight and EpCam^{+}Lgr5^{+} cells together with drastically enhanced T cell activation and immune cell infiltration in the tumor compared to control bacteria (fig. S17, H to L). These results suggested that bacterial co-therapy may optimize treatment regimens in MMRD tumors. Notably, anti-IL-12p75 treatment almost completely abrogated the effect of ICB-promoting, anti-CTLA-4 co-therapy in *Msh2$^{LoxP/LoxP}$Villin-Cre* tumors (fig. S17, G to L), which supports a critical role for inosine-dependent up-regulation of IL12Rβ2 on T cells and cDC production of IL-12 and corroborates similar findings upon simultaneous depletion of IL-12 and IL-23, using anti-IL-12p40 treatment (*6*, *8*). Since oxaliplatin/anti-PD-L1 co-treatment is a more commonly used therapy in the clinics, we also confirmed that ICB-promoting bacteria enhanced the efficacy of oxaliplatin/anti-PD-L1 co-treatment in SPF *Msh2$^{LoxP/LoxP}$Villin-Cre animals* (fig. S18).

As *B. pseudolongum* was enriched in AOM/DSS tumors of ICB-treated animals (Fig. 1, F and G) and *Bifidobacteria* were previously associated with improved ICB-therapy efficacy in cancer patients (*9*), we wondered whether *Bifidobacteria* were also enriched in *Msh2$^{LoxP/LoxP}$Villin-Cre* tumors of ICB-treated mice. While the total amount of tumor-associated bacteria in did not change with anti-CTLA-4 or anti-PD-L1 treatment (fig. S19A), ICB treatment led to specific enrichment of tumor-associated *Bifidobacteria* (fig. S19B). Intriguingly, a recent report revealed that compared to other tissues, *Bifidobacteria* colonize tumors, likely due to the hypoxic environment often found in tumors (*41*). At this point it is unclear why *Bifidobacteria* seem to preferentially do so in ICB-treated conditions.

We next tested the ICB-promoting effect of *B. pseudolongum*, *L. johnsonii* and *Olsenella* species in SPF *Apc$^{2lox14/+}$;Kras$^{LSL-G12D/+}$;Fabpl-Cre* (*42*) mice, which have conditional *Apc* deficiency and activation of *Kras* specifically in colonocytes. In this model of CRC, anti-CTLA-4 treatment did not improve survival compared to isotype-treated animals (fig. S20, A and B), and transfer of the ICB-promoting bacteria failed to enhance survival (fig. S20, C and D), revealing a limitation of bacterial co-therapy in this model.

Finally, we tested whether the bacterial metabolite inosine in combination with co-stimulation was sufficient to enhance the efficacy of ICB therapy in other cancer models. Oral administration of inosine together with anti-CTLA-4 and CpG treatment in SPF *Msh2$^{LoxP/LoxP}$Villin-Cre* mice led to significant reduction in tumor weight and a corresponding increase in splenic IFN-γ^{+}CD4^{+} and IFN-γ^{+}CD8^{+} T cells (Fig. 4, A to F). Importantly, inosine together with CpG was also found to be effective in promoting the efficacy of anti-CTLA-4 in two additional murine cancers—bladder cancer and melanoma. Specifically, inosine plus CpG administration to GF mice that had been injected with MB49 murine bladder cancer cells was able to significantly enhance the ability of anti-CTLA-4 to reduce tumor weights and increase the proportion of IFN-γ^{+}CD4^{+} and IFN-γ^{+}CD8^{+} T cells infiltrating the tumors (Fig. 4, G to K). Similarly, inosine plus CpG augmented the ability of anti-CTLA-4 to mediate anti-tumor immunity in a heterotopic mouse model of melanoma (Fig. 4, L to P).

In summary, our results identify a *B. pseudolongum* strain isolated from ICB-treated CRC tumors as a key commensal intestinal bacterial species that is capable of boosting a cDC-dependent Th1 cell circuit to greatly enhance the effect of ICB therapies in mouse models of intestinal and epithelial tumors (fig. S21). These data support the premise that modification of the microbiota or targeted bacterial therapies with defined microbial consortia may provide a promising adjuvant therapy to ICB in CRC and other cancers. Although isolated from mice, all three ICB-promoting bacteria are also found in humans, indicating their potential for translation (*43*–*45*). Furthermore, we analyzed published human fecal microbiome metagenomic datasets (*8*, *9*, *46*) and found a trend, although not significant, where *B. pseudolongum* was enriched [up to 2.4-fold; (*8*)] in responders compared to nonresponding cancer patients (fig. S22A). At the genus level, *Bifidobacteria* were also enriched (albeit non-significantly) in responders versus nonresponders [5.9-fold; fig. S22B (*9*)], with the species *B. longum* and *B. adolescentis* significantly enriched (*47*). Due to the low abundance of *B. pseudolongum* in fecal samples of adults, higher powered studies with larger sample sizes will be needed to confirm this trend. We also identified inosine as a key bacterial-derived metabolite acting through T cell-specific $A_{2A}R$ signaling to promote Th1 cell activation in a context-dependent manner. We further confirmed that *A. muciniphila*, which is known to be associated with responsiveness to ICB therapy in humans (*8*), utilizes inosine-$A_{2A}R$ signaling for its ICB-promoting effect. In light of our findings, one might caution against the blockade of inosine-$A2_A$ receptor signaling for cancer immunotherapy as this may negate any positive effect provided by beneficial microbes. We suggest that $A2_A$ receptor signaling is likely an integral anti-tumor pathway for bacterial-ICB co-therapies. Further investigation of the effects of xanthine and hypoxanthine, degradation products of inosine, are warranted.

REFERENCES AND NOTES

1. F. S. Hodi, S. J. O'Day, D. F. McDermott, R. W. Weber, J. A. Sosman, J. B. Haanen, R. Gonzalez, C. Robert, D. Schadendorf, J. C. Hassel, W. Akerley, A. J. M. van den Eertwegh, J. Lutzky, P. Lorigan, J. M. Vaubel, G. P. Linette, D. Hogg, C. H. Ottensmeier, C. Lebbé, C. Peschel, I. Quirt, J. I. Clark, J. D. Wolchok, J. S. Weber, J. Tian, M. J. Yellin, G. M. Nichol, A. Hoos, W. J. Urba, Improved survival with ipilimumab in patients with metastatic melanoma. *N. Engl. J. Med.* **363**, 711–723 (2010). doi:10.1056/NEJMoa1003466 Medline

2. J. R. Brahmer, S. S. Tykodi, L. Q. M. Chow, W.-J. Hwu, S. L. Topalian, P. Hwu, C. G. Drake, L. H. Camacho, J. Kauh, K. Odunsi, H. C. Pitot, O. Hamid, S. Bhatia, R. Martins, K. Eaton, S. Chen, T. M. Salay, S. Alaparthy, J. F. Grosso, A. J. Korman, S. M. Parker, S. Agrawal, S. M. Goldberg, D. M. Pardoll, A. Gupta, J. M. Wigginton, Safety and activity of anti-PD-L1 antibody in patients with advanced cancer. *N. Engl. J. Med.* **366**, 2455–2465 (2012). doi:10.1056/NEJMoa1200694 Medline
3. R. J. Motzer, B. Escudier, D. F. McDermott, S. George, H. J. Hammers, S. Srinivas, S. S. Tykodi, J. A. Sosman, G. Procopio, E. R. Plimack, D. Castellano, T. K. Choueiri, H. Gurney, F. Donskov, P. Bono, J. Wagstaff, T. C. Gauler, T. Ueda, Y. Tomita, F. A. Schutz, C. Kollmannsberger, J. Larkin, A. Ravaud, J. S. Simon, L.-A. Xu, I. M. Waxman, P. Sharma; CheckMate 025 Investigators, Nivolumab versus everolimus in advanced renal-cell carcinoma. *N. Engl. J. Med.* **373**, 1803–1813 (2015). doi:10.1056/NEJMoa1510665 Medline
4. H. Borghaei, L. Paz-Ares, L. Horn, D. R. Spigel, M. Steins, N. E. Ready, L. Q. Chow, E. E. Vokes, E. Felip, E. Holgado, F. Barlesi, M. Kohlhäufl, O. Arrieta, M. A. Burgio, J. Fayette, H. Lena, E. Poddubskaya, D. E. Gerber, S. N. Gettinger, C. M. Rudin, N. Rizvi, L. Crinò, G. R. Blumenschein Jr., S. J. Antonia, C. Dorange, C. T. Harbison, F. Graf Finckenstein, J. R. Brahmer, Nivolumab versus docetaxel in advanced nonsquamous non-small-cell lung cancer. *N. Engl. J. Med.* **373**, 1627–1639 (2015). doi:10.1056/NEJMoa1507643 Medline
5. T. N. Gide, J. S. Wilmott, R. A. Scolyer, G. V. Long, Primary and acquired resistance to immune checkpoint inhibitors in metastatic melanoma. *Clin. Cancer Res.* **24**, 1260–1270 (2018). doi:10.1158/1078-0432.CCR-17-2267 Medline
6. M. Vétizou, J. M. Pitt, R. Daillère, P. Lepage, N. Waldschmitt, C. Flament, S. Rusakiewicz, B. Routy, M. P. Roberti, C. P. M. Duong, V. Poirier-Colame, A. Roux, S. Becharef, S. Formenti, E. Golden, S. Cording, G. Eberl, A. Schlitzer, F. Ginhoux, S. Mani, T. Yamazaki, N. Jacquelot, D. P. Enot, M. Bérard, J. Nigou, P. Opolon, A. Eggermont, P.-L. Woerther, E. Chachaty, N. Chaput, C. Robert, C. Mateus, G. Kroemer, D. Raoult, I. G. Boneca, F. Carbonnel, M. Chamaillard, L. Zitvogel, Anticancer immunotherapy by CTLA-4 blockade relies on the gut microbiota. *Science* **350**, 1079–1084 (2015). doi:10.1126/science.aad1329 Medline
7. A. Sivan, L. Corrales, N. Hubert, J. B. Williams, K. Aquino-Michaels, Z. M. Earley, F. W. Benyamin, Y. M. Lei, B. Jabri, M.-L. Alegre, E. B. Chang, T. F. Gajewski, Commensal *Bifidobacterium* promotes antitumor immunity and facilitates anti-PD-L1 efficacy. *Science* **350**, 1084–1089 (2015). doi:10.1126/science.aac4255 Medline
8. B. Routy, E. Le Chatelier, L. Derosa, C. P. M. Duong, M. T. Alou, R. Daillère, A. Fluckiger, M. Messaoudene, C. Rauber, M. P. Roberti, M. Fidelle, C. Flament, V. Poirier-Colame, P. Opolon, C. Klein, K. Iribarren, L. Mondragón, N. Jacquelot, B. Qu, G. Ferrere, C. Clémenson, L. Mezquita, J. R. Masip, C. Naltet, S. Brosseau, C. Kaderbhai, C. Richard, H. Rizvi, F. Levenez, N. Galleron, B. Quinquis, N. Pons, B. Ryffel, V. Minard-Colin, P. Gonin, J.-C. Soria, E. Deutsch, Y. Loriot, F. Ghiringhelli, G. Zalcman, F. Goldwasser, B. Escudier, M. D. Hellmann, A. Eggermont, D. Raoult, L. Albiges, G. Kroemer, L. Zitvogel, Gut microbiome influences efficacy of PD-1-based immunotherapy against epithelial tumors. *Science* **359**, 91–97 (2018). doi:10.1126/science.aan3706 Medline
9. V. Matson, J. Fessler, R. Bao, T. Chongsuwat, Y. Zha, M.-L. Alegre, J. J. Luke, T. F. Gajewski, The commensal microbiome is associated with anti-PD-1 efficacy in metastatic melanoma patients. *Science* **359**, 104–108 (2018). doi:10.1126/science.aao3290 Medline
10. V. Gopalakrishnan, C. N. Spencer, L. Nezi, A. Reuben, M. C. Andrews, T. V. Karpinets, P. A. Prieto, D. Vicente, K. Hoffman, S. C. Wei, A. P. Cogdill, L. Zhao, C. W. Hudgens, D. S. Hutchinson, T. Manzo, M. Petaccia de Macedo, T. Cotechini, T. Kumar, W. S. Chen, S. M. Reddy, R. Szczepaniak Sloane, J. Galloway-Pena, H. Jiang, P. L. Chen, E. J. Shpall, K. Rezvani, A. M. Alousi, R. F. Chemaly, S. Shelburne, L. M. Vence, P. C. Okhuysen, V. B. Jensen, A. G. Swennes, F. McAllister, E. Marcelo Riquelme Sanchez, Y. Zhang, E. Le Chatelier, L. Zitvogel, N. Pons, J. L. Austin-Breneman, L. E. Haydu, E. M. Burton, J. M. Gardner, E. Sirmans, J. Hu, A. J. Lazar, T. Tsujikawa, A. Diab, H. Tawbi, I. C. Glitza, W. J. Hwu, S. P. Patel, S. E. Woodman, R. N. Amaria, M. A. Davies, J. E. Gershenwald, P. Hwu, J. E. Lee, J. Zhang, L. M. Coussens, Z. A. Cooper, P. A. Futreal, C. R. Daniel, N. J. Ajami, J. F. Petrosino, M. T. Tetzlaff, P. Sharma, J. P. Allison, R. R. Jenq, J. A. Wargo, Gut microbiome modulates response to anti-PD-1 immunotherapy in melanoma patients. *Science* **359**, 97–103 (2018). doi:10.1126/science.aan4236 Medline
11. C. M. Dejea, P. Fathi, J. M. Craig, A. Boleij, R. Taddese, A. L. Geis, X. Wu, C. E. DeStefano Shields, E. M. Hechenbleikner, D. L. Huso, R. A. Anders, F. M. Giardiello, E. C. Wick, H. Wang, S. Wu, D. M. Pardoll, F. Housseau, C. L. Sears, Patients with familial adenomatous polyposis harbor colonic biofilms containing tumorigenic bacteria. *Science* **359**, 592–597 (2018). doi:10.1126/science.aah3648 Medline
12. J. C. Arthur, E. Perez-Chanona, M. Mühlbauer, S. Tomkovich, J. M. Uronis, T.-J. Fan, B. J. Campbell, T. Abujamel, B. Dogan, A. B. Rogers, J. M. Rhodes, A. Stintzi, K. W. Simpson, J. J. Hansen, T. O. Keku, A. A. Fodor, C. Jobin, Intestinal inflammation targets cancer-inducing activity of the microbiota. *Science* **338**, 120–123 (2012). doi:10.1126/science.1224820 Medline
13. N. Iida, A. Dzutsev, C. A. Stewart, L. Smith, N. Bouladoux, R. A. Weingarten, D. A. Molina, R. Salcedo, T. Back, S. Cramer, R.-M. Dai, H. Kiu, M. Cardone, S. Naik, A. K. Patri, E. Wang, F. M. Marincola, K. M. Frank, Y. Belkaid, G. Trinchieri, R. S. Goldszmid, Commensal bacteria control cancer response to therapy by modulating the tumor microenvironment. *Science* **342**, 967–970 (2013). doi:10.1126/science.1240527 Medline
14. S. Viaud, F. Saccheri, G. Mignot, T. Yamazaki, R. Daillère, D. Hannani, D. P. Enot, C. Pfirschke, C. Engblom, M. J. Pittet, A. Schlitzer, F. Ginhoux, L. Apetoh, E. Chachaty, P.-L. Woerther, G. Eberl, M. Bérard, C. Ecobichon, D. Clermont, C. Bizet, V. Gaboriau-Routhiau, N. Cerf-Bensussan, P. Opolon, N. Yessaad, E. Vivier, B. Ryffel, C. O. Elson, J. Doré, G. Kroemer, P. Lepage, I. G. Boneca, F. Ghiringhelli, L. Zitvogel, The intestinal microbiota modulates the anticancer immune effects of cyclophosphamide. *Science* **342**, 971–976 (2013). doi:10.1126/science.1240537 Medline
15. D. T. Le, J. N. Uram, H. Wang, B. R. Bartlett, H. Kemberling, A. D. Eyring, A. D. Skora, B. S. Luber, N. S. Azad, D. Laheru, B. Biedrzycki, R. C. Donehower, A. Zaheer, G. A. Fisher, T. S. Crocenzi, J. J. Lee, S. M. Duffy, R. M. Goldberg, A. de la Chapelle, M. Koshiji, F. Bhaijee, T. Huebner, R. H. Hruban, L. D. Wood, N. Cuka, D. M. Pardoll, N. Papadopoulos, K. W. Kinzler, S. Zhou, T. C. Cornish, J. M. Taube, R. A. Anders, J. R. Eshleman, B. Vogelstein, L. A. Diaz Jr., PD-1 blockade in tumors with mismatch-repair deficiency. *N. Engl. J. Med.* **372**, 2509–2520 (2015). doi:10.1056/NEJMoa1500596 Medline
16. S. C. Wei, J. H. Levine, A. P. Cogdill, Y. Zhao, N. A. S. Anang, M. C. Andrews, P. Sharma, J. Wang, J. A. Wargo, D. Pe'er, J. P. Allison, Distinct cellular mechanisms underlie anti-CTLA-4 and anti-PD-1 checkpoint blockade. *Cell* **170**, 1120–1133.e17 (2017). doi:10.1016/j.cell.2017.07.024 Medline
17. K. A. Ward-Hartstonge, R. A. Kemp, Regulatory T-cell heterogeneity and the cancer immune response. *Clin. Transl. Immunology* **6**, e154 (2017). doi:10.1038/cti.2017.43 Medline
18. R. F. Schwabe, C. Jobin, The microbiome and cancer. *Nat. Rev. Cancer* **13**, 800–812 (2013). doi:10.1038/nrc3610 Medline
19. G. A. Lugli, S. Duranti, K. Albert, L. Mancabelli, S. Napoli, A. Viappiani, R. Anzalone, G. Longhi, C. Milani, F. Turroni, G. Alessandri, D. A. Sela, D. van Sinderen, M. Ventura, Unveiling genomic diversity among members of the species *Bifidobacterium pseudolongum*, a widely distributed gut commensal of the animal kingdom. *Appl. Environ. Microbiol.* **85**, e03065-18 (2019). doi:10.1128/AEM.03065-18 Medline
20. D. W. Zheng, Y. Chen, Z.-H. Li, L. Xu, C.-X. Li, B. Li, J.-X. Fan, S.-X. Cheng, X.-Z. Zhang, Optically-controlled bacterial metabolite for cancer therapy. *Nat. Commun.* **9**, 1680 (2018). doi:10.1038/s41467-018-03233-9 Medline
21. T. Tanoue, S. Morita, D. R. Plichta, A. N. Skelly, W. Suda, Y. Sugiura, S. Narushima, H. Vlamakis, I. Motoo, K. Sugita, A. Shiota, K. Takeshita, K. Yasuma-Mitobe, D. Riethmacher, T. Kaisho, J. M. Norman, D. Mucida, M. Suematsu, T. Yaguchi, V. Bucci, T. Inoue, Y. Kawakami, B. Olle, B. Roberts, M. Hattori, R. J. Xavier, K. Atarashi, K. Honda, A defined commensal consortium elicits CD8 T cells and anti-cancer immunity. *Nature* **565**, 600–605 (2019). doi:10.1038/s41586-019-0878-z Medline
22. F. Wang, Q. Yin, L. Chen, M. M. Davis, *Bifidobacterium* can mitigate intestinal immunopathology in the context of CTLA-4 blockade. *Proc. Natl. Acad. Sci. U.S.A.* **115**, 157–161 (2018). doi:10.1073/pnas.1712901115 Medline
23. A. A. Welihinda, M. Kaur, K. Greene, Y. Zhai, E. P. Amento, The adenosine metabolite inosine is a functional agonist of the adenosine A2A receptor with a unique signaling bias. *Cell. Signal.* **28**, 552–560 (2016). doi:10.1016/j.cellsig.2016.02.010 Medline
24. G. Haskó, D. G. Kuhel, Z. H. Németh, J. G. Mabley, R. F. Stachlewitz, L. Virág, Z. Lohinai, G. J. Southan, A. L. Salzman, C. Szabó, Inosine inhibits inflammatory

cytokine production by a posttranscriptional mechanism and protects against endotoxin-induced shock. *J. Immunol.* **164**, 1013–1019 (2000). doi:10.4049/jimmunol.164.2.1013 Medline

25. B. He, T. K. Hoang, T. Wang, M. Ferris, C. M. Taylor, X. Tian, M. Luo, D. Q. Tran, J. Zhou, N. Tatevian, F. Luo, J. G. Molina, M. R. Blackburn, T. H. Gomez, S. Roos, J. M. Rhoads, Y. Liu, Resetting microbiota by *Lactobacillus reuteri* inhibits T reg deficiency–induced autoimmunity via adenosine A_{2A} receptors. *J. Exp. Med.* **214**, 107–123 (2017). doi:10.1084/jem.20160961 Medline
26. B. Csóka, L. Himer, Z. Selmeczy, E. S. Vizi, P. Pacher, C. Ledent, E. A. Deitch, Z. Spolarics, Z. H. Németh, G. Haskó, Adenosine A_{2A} receptor activation inhibits T helper 1 and T helper 2 cell development and effector function. *FASEB J.* **22**, 3491–3499 (2008). doi:10.1096/fj.08-107458 Medline
27. A. Ohta, E. Gorelik, S. J. Prasad, F. Ronchese, D. Lukashev, M. K. K. Wong, X. Huang, S. Caldwell, K. Liu, P. Smith, J.-F. Chen, E. K. Jackson, S. Apasov, S. Abrams, M. Sitkovsky, A2A adenosine receptor protects tumors from antitumor T cells. *Proc. Natl. Acad. Sci. U.S.A.* **103**, 13132–13137 (2006). doi:10.1073/pnas.0605251103 Medline
28. S. Vigano, D. Alatzoglou, M. Irving, C. Ménétrier-Caux, C. Caux, P. Romero, G. Coukos, Targeting adenosine in cancer immunotherapy to enhance T-cell function. *Front. Immunol.* **10**, 925 (2019). doi:10.3389/fimmu.2019.00925 Medline
29. C. Cekic, J. Linden, Adenosine A_{2A} receptors intrinsically regulate $CD8^+$ T cells in the tumor microenvironment. *Cancer Res.* **74**, 7239–7249 (2014). doi:10.1158/0008-5472.CAN-13-3581 Medline
30. W. Lasek, M. Janyst, R. Wolny, Ł. Zapała, K. Bocian, N. Drela, Immunomodulatory effects of inosine pranobex on cytokine production by human lymphocytes. *Acta Pharm.* **65**, 171–180 (2015). doi:10.1515/acph-2015-0015 Medline
31. T. Lioux, M.-A. Mauny, A. Lamoureux, N. Bascoul, M. Hays, F. Vernejoul, A.-S. Baudru, C. Boularan, J. Lopes-Vicente, G. Qushair, G. Tiraby, Design, synthesis, and biological evaluation of novel cyclic adenosine-inosine monophosphate (cAIMP) analogs that activate stimulator of interferon genes (STING). *J. Med. Chem.* **59**, 10253–10267 (2016). doi:10.1021/acs.jmedchem.6b01300 Medline
32. C. Yao, T. Hirata, K. Soontrapa, X. Ma, H. Takemori, S. Narumiya, Prostaglandin E_2 promotes Th1 differentiation via synergistic amplification of IL-12 signalling by cAMP and PI3-kinase. *Nat. Commun.* **4**, 1685 (2013). doi:10.1038/ncomms2684 Medline
33. B. Samten, J. C. Townsend, S. E. Weis, A. Bhoumik, P. Klucar, H. Shams, P. F. Barnes, CREB, ATF, and AP-1 transcription factors regulate IFN-γ secretion by human T cells in response to mycobacterial antigen. *J. Immunol.* **181**, 2056–2064 (2008). doi:10.4049/jimmunol.181.3.2056 Medline
34. B. Samten, S. T. Howard, S. E. Weis, S. Wu, H. Shams, J. C. Townsend, H. Safi, P. F. Barnes, Cyclic AMP response element-binding protein positively regulates production of IFN-γ by T cells in response to a microbial pathogen. *J. Immunol.* **174**, 6357–6363 (2005). doi:10.4049/jimmunol.174.10.6357 Medline
35. B. Jahrsdörfer, G. J. Weiner, CpG oligodeoxynucleotides as immunotherapy in cancer. *Update Cancer Ther.* **3**, 27–32 (2008). doi:10.1016/j.uct.2007.11.003 Medline
36. S. Brugiroux, M. Beutler, C. Pfann, D. Garzetti, H.-J. Ruscheweyh, D. Ring, M. Diehl, S. Herp, Y. Lötscher, S. Hussain, B. Bunk, R. Pukall, D. H. Huson, P. C. Münch, A. C. McHardy, K. D. McCoy, A. J. Macpherson, A. Loy, T. Clavel, D. Berry, B. Stecher, Genome-guided design of a defined mouse microbiota that confers colonization resistance against *Salmonella enterica* serovar Typhimurium. *Nat. Microbiol.* **2**, 16215 (2016). doi:10.1038/nmicrobiol.2016.215 Medline
37. C. S. Garris, S. P. Arlauckas, R. H. Kohler, M. P. Trefny, S. Garren, C. Piot, C. Engblom, C. Pfirschke, M. Siwicki, J. Gungabeesoon, G. J. Freeman, S. E. Warren, S. Ong, E. Browning, C. G. Twitty, R. H. Pierce, M. H. Le, A. P. Algazi, A. I. Daud, S. I. Pai, A. Zippelius, R. Weissleder, M. J. Pittet, Successful anti-PD-1 cancer immunotherapy requires T cell-dendritic cell crosstalk involving the cytokines IFN-γ and IL-12. *Immunity* **49**, 1148–1161.e7 (2018). doi:10.1016/j.immuni.2018.09.024 Medline
38. D. Chraa, A. Naim, D. Olive, A. Badou, T lymphocyte subsets in cancer immunity: Friends or foes. *J. Leukoc. Biol.* **105**, 243–255 (2019). doi:10.1002/JLB.MR0318-097R Medline
39. M. H. Kucherlapati, K. Lee, A. A. Nguyen, A. B. Clark, H. Hou Jr., A. Rosulek, H. Li, K. Yang, K. Fan, M. Lipkin, R. T. Bronson, L. Jelicks, T. A. Kunkel, R. Kucherlapati, W. Edelmann, An *Msh2* conditional knockout mouse for studying intestinal cancer and testing anticancer agents. *Gastroenterology* **138**, 993–1002.e1 (2010). doi:10.1053/j.gastro.2009.11.009 Medline
40. D. T. Le, J. N. Durham, K. N. Smith, H. Wang, B. R. Bartlett, L. K. Aulakh, S. Lu, H. Kemberling, C. Wilt, B. S. Luber, F. Wong, N. S. Azad, A. A. Rucki, D. Laheru, R. Donehower, A. Zaheer, G. A. Fisher, T. S. Crocenzi, J. J. Lee, T. F. Greten, A. G. Duffy, K. K. Ciombor, A. D. Eyring, B. H. Lam, A. Joe, S. P. Kang, M. Holdhoff, L. Danilova, L. Cope, C. Meyer, S. Zhou, R. M. Goldberg, D. K. Armstrong, K. M. Bever, A. N. Fader, J. Taube, F. Housseau, D. Spetzler, N. Xiao, D. M. Pardoll, N. Papadopoulos, K. W. Kinzler, J. R. Eshleman, B. Vogelstein, R. A. Anders, L. A. Diaz Jr., Mismatch repair deficiency predicts response of solid tumors to PD-1 blockade. *Science* **357**, 409–413 (2017). doi:10.1126/science.aan6733 Medline
41. Y. Shi, W. Zheng, K. Yang, K. G. Harris, K. Ni, L. Xue, W. Lin, E. B. Chang, R. R. Weichselbaum, Y.-X. Fu, Intratumoral accumulation of gut microbiota facilitates CD47-based immunotherapy via STING signaling. *J. Exp. Med.* **217**, e20192282 (2020). doi:10.1084/jem.20192282 Medline
42. K. M. Haigis, K. R. Kendall, Y. Wang, A. Cheung, M. C. Haigis, J. N. Glickman, M. Niwa-Kawakita, A. Sweet-Cordero, J. Sebolt-Leopold, K. M. Shannon, J. Settleman, M. Giovannini, T. Jacks, Differential effects of oncogenic K-Ras and N-Ras on proliferation, differentiation and tumor progression in the colon. *Nat. Genet.* **40**, 600–608 (2008). doi:10.1038/ng.115 Medline
43. F. Turroni, E. Foroni, P. Pizzetti, V. Giubellini, A. Ribbera, P. Merusi, P. Cagnasso, B. Bizzarri, G. L. de'Angelis, F. Shanahan, D. van Sinderen, M. Ventura, Exploring the diversity of the bifidobacterial population in the human intestinal tract. *Appl. Environ. Microbiol.* **75**, 1534–1545 (2009). doi:10.1128/AEM.02216-08 Medline
44. R. D. Pridmore, A. C. Pittet, F. Praplan, C. Cavadini, Hydrogen peroxide production by *Lactobacillus johnsonii* NCC 533 and its role in anti-*Salmonella* activity. *FEMS Microbiol. Lett.* **283**, 210–215 (2008). doi:10.1111/j.1574-6968.2008.01176.x Medline
45. F. E. Dewhirst, B. J. Paster, N. Tzellas, B. Coleman, J. Downes, D. A. Spratt, W. G. Wade, Characterization of novel human oral isolates and cloned 16S rDNA sequences that fall in the family *Coriobacteriaceae*: Description of *Olsenella* gen. nov., reclassification of *Lactobacillus uli* as *Olsenella uli* comb. nov. and description of *Olsenella profusa* sp. nov. *Int. J. Syst. Evol. Microbiol.* **51**, 1797–1804 (2001). doi:10.1099/00207713-51-5-1797 Medline
46. A. E. Frankel, L. A. Coughlin, J. Kim, T. W. Froehlich, Y. Xie, E. P. Frenkel, A. Y. Koh, Metagenomic shotgun sequencing and unbiased metabolomic profiling identify specific human gut microbiota and metabolites associated with immune checkpoint therapy efficacy in melanoma patients. *Neoplasia* **19**, 848–855 (2017). doi:10.1016/j.neo.2017.08.004 Medline
47. B. A. Helmink, M. A. W. Khan, A. Hermann, V. Gopalakrishnan, J. A. Wargo, The microbiome, cancer, and cancer therapy. *Nat. Med.* **25**, 377–388 (2019). doi:10.1038/s41591-019-0377-7 Medline
48. M. M. Meredith, K. Liu, G. Darrasse-Jeze, A. O. Kamphorst, H. A. Schreiber, P. Guermonprez, J. Idoyaga, C. Cheong, K.-H. Yao, R. E. Niec, M. C. Nussenzweig, Expression of the zinc finger transcription factor zDC (Zbtb46, Btbd4) defines the classical dendritic cell lineage. *J. Exp. Med.* **209**, 1153–1165 (2012). doi:10.1084/jem.20112675 Medline
49. K. A. Hogquist, S. C. Jameson, W. R. Heath, J. L. Howard, M. J. Bevan, F. R. Carbone, T cell receptor antagonist peptides induce positive selection. *Cell* **76**, 17–27 (1994). doi:10.1016/0092-8674(94)90169-4 Medline
50. M. J. Barnden, J. Allison, W. R. Heath, F. R. Carbone, Defective TCR expression in transgenic mice constructed using cDNA-based α- and β-chain genes under the control of heterologous regulatory elements. *Immunol. Cell Biol.* **76**, 34–40 (1998). doi:10.1046/j.1440-1711.1998.00709.x Medline
51. B. Allard, I. Cousineau, D. Allard, L. Buisseret, S. Pommey, P. Chrobak, J. Stagg, Adenosine A2a receptor promotes lymphangiogenesis and lymph node metastasis. *OncoImmunology* **8**, 1601481 (2019). doi:10.1080/2162402X.2019.1601481 Medline
52. L. F. Mager, V. H. Koelzer, R. Stuber, L. Thoo, I. Keller, I. Koeck, M. Langenegger, C. Simillion, S. P. Pfister, M. Faderl, V. Genitsch, I. Tcymbarevich, P. Juillerat, X. Li, Y. Xia, E. Karamitopoulou, R. Lyck, I. Zlobec, S. Hapfelmeier, R. Bruggmann, K. D. McCoy, A. J. Macpherson, C. Müller, B. Beutler, P. Krebs, The ESRP1-GPR137 axis contributes to intestinal pathogenesis. *eLife* **6**, e28366 (2017). doi:10.7554/eLife.28366 Medline

53. K. D. Mertz, L. F. Mager, M.-H. Wasmer, T. Thiesler, V. H. Koelzer, G. Ruzzante, S. Joller, J. R. Murdoch, T. Brümmendorf, V. Genitsch, A. Lugli, G. Cathomas, H. Moch, A. Weber, I. Zlobec, T. Junt, P. Krebs, The IL-33/ST2 pathway contributes to intestinal tumorigenesis in humans and mice. *OncoImmunology* **5**, e1062966 (2016). doi:10.1080/2162402X.2015.1062966 Medline
54. J. J. Kozich, S. L. Westcott, N. T. Baxter, S. K. Highlander, P. D. Schloss, Development of a dual-index sequencing strategy and curation pipeline for analyzing amplicon sequence data on the MiSeq Illumina sequencing platform. *Appl. Environ. Microbiol.* **79**, 5112–5120 (2013). doi:10.1128/AEM.01043-13 Medline
55. B. J. Callahan, P. J. McMurdie, M. J. Rosen, A. W. Han, A. J. A. Johnson, S. P. Holmes, DADA2: High-resolution sample inference from Illumina amplicon data. *Nat. Methods* **13**, 581–583 (2016). doi:10.1038/nmeth.3869 Medline
56. T. Z. DeSantis, P. Hugenholtz, N. Larsen, M. Rojas, E. L. Brodie, K. Keller, T. Huber, D. Dalevi, P. Hu, G. L. Andersen, Greengenes, a chimera-checked 16S rRNA gene database and workbench compatible with ARB. *Appl. Environ. Microbiol.* **72**, 5069–5072 (2006). doi:10.1128/AEM.03006-05 Medline
57. M. I. Love, W. Huber, S. Anders, Moderated estimation of fold change and dispersion for RNA-seq data with DESeq2. *Genome Biol.* **15**, 550 (2014). doi:10.1186/s13059-014-0550-8 Medline
58. K. P. Schliep, phangorn: Phylogenetic analysis in R. *Bioinformatics* **27**, 592–593 (2011). doi:10.1093/bioinformatics/btq706 Medline
59. J. Lloyd-Price, C. Arze, A. N. Ananthakrishnan, M. Schirmer, J. Avila-Pacheco, T. W. Poon, E. Andrews, N. J. Ajami, K. S. Bonham, C. J. Brislawn, D. Casero, H. Courtney, A. Gonzalez, T. G. Graeber, A. B. Hall, K. Lake, C. J. Landers, H. Mallick, D. R. Plichta, M. Prasad, G. Rahnavard, J. Sauk, D. Shungin, Y. Vázquez-Baeza, R. A. White 3rd, J. Braun, L. A. Denson, J. K. Jansson, R. Knight, S. Kugathasan, D. P. B. McGovern, J. F. Petrosino, T. S. Stappenbeck, H. S. Winter, C. B. Clish, E. A. Franzosa, H. Vlamakis, R. J. Xavier, C. Huttenhower; IBDMDB Investigators, Multi-omics of the gut microbial ecosystem in inflammatory bowel diseases. *Nature* **569**, 655–662 (2019). doi:10.1038/s41586-019-1237-9 Medline
60. W. G. Weisburg, S. M. Barns, D. A. Pelletier, D. J. Lane, 16S ribosomal DNA amplification for phylogenetic study. *J. Bacteriol.* **173**, 697–703 (1991). doi:10.1128/JB.173.2.697-703.1991 Medline
61. L. F. Mager, C. Riether, C. M. Schürch, Y. Banz, M.-H. Wasmer, R. Stuber, A. P. Theocharides, X. Li, Y. Xia, H. Saito, S. Nakae, G. M. Baerlocher, M. G. Manz, K. D. McCoy, A. J. Macpherson, A. F. Ochsenbein, B. Beutler, P. Krebs, IL-33 signaling contributes to the pathogenesis of myeloproliferative neoplasms. *J. Clin. Invest.* **125**, 2579–2591 (2015). doi:10.1172/JCI77347 Medline
62. H. Gowda, J. Ivanisevic, C. H. Johnson, M. E. Kurczy, H. P. Benton, D. Rinehart, T. Nguyen, J. Ray, J. Kuehl, B. Arevalo, P. D. Westenskow, J. Wang, A. P. Arkin, A. M. Deutschbauer, G. J. Patti, G. Siuzdak, Interactive XCMS Online: Simplifying advanced metabolomic data processing and subsequent statistical analyses. *Anal. Chem.* **86**, 6931–6939 (2014). doi:10.1021/ac500734c Medline
63. R. Tautenhahn, G. J. Patti, D. Rinehart, G. Siuzdak, XCMS Online: A web-based platform to process untargeted metabolomic data. *Anal. Chem.* **84**, 5035–5039 (2012). doi:10.1021/ac300698c Medline
64. M. F. Clasquin, E. Melamud, J. D. Rabinowitz, LC-MS data processing with MAVEN: A metabolomic analysis and visualization engine. *Curr. Protoc. Bioinformatics* **37**, 14.11.1–14.11.23 (2012). Medline
65. E. Melamud, L. Vastag, J. D. Rabinowitz, Metabolomic analysis and visualization engine for LC-MS data. *Anal. Chem.* **82**, 9818–9826 (2010). doi:10.1021/ac1021166 Medline

ACKNOWLEDGMENTS

We are grateful to C. Thomson, A. Ignacio Silvestre da Silva, M. Wyss, M. Davoli-Ferreira, J. Yee and M. Koegler for their help in tackling large scale experiments, their technical knowledge and critical feedback. We thank M. Dicay for performing the Ussing chamber experiments. **Funding:** L.F.M. was supported by the Early Postdoc Mobility Fellowship from the Swiss National Science Foundation. K.D.M. is supported by a Canadian Institutes of Health Research (CIHR) grant (PJT-165930), a Canadian Foundation for Innovation (CFI) John R. Evans Leaders Fund (JELF) grant, the Cumming School of Medicine, and the Carole May Yates Memorial Endowment for Cancer Research. M.B.G. is supported by CIHR (PJT-156073) and CFI-JELF. R.A.G. is supported by a CFI-JELF (#34986) and the International Microbiome Centre (IMC). K.B. is supported by a Canada Graduate Scholarship from the Natural Sciences and Engineering Research Council of Canada (NSERC). I.A.L. is supported by an Alberta Innovates Translational Health Chair. J.S. is supported by a CIHR grant and a Terry Fox Research Institute grant. The IMC is supported by the Cumming School of Medicine, University of Calgary, Western Economic Diversification (WED) and Alberta Economic Development and Trade (AEDT), Canada. **Author contributions:** L.F.M., R.B., N.P., N.C., K.B., H.R., S.P., R.A.G., I.A.L., and M.G. performed experiments and analyzed data. L.F.M., M.B.G. and K.D.M. wrote the manuscript, and all authors revised the manuscript and approved its final version. J.S. provided $A_{2A}R$-deficient mice. L.F.M. and K.D.M. conceived the project. K.D.M. and M.B.G. supervised the project. **Competing interests:** J.S. is a permanent member of the Scientific Advisory Board of Surface Oncology and owns stocks of Surface Oncology. L.F.M. and K.D.M. are inventors on patent US 62/929,340 submitted by UTI Limited Partnership that covers the use of bacterial species and inosine as immune checkpoint blockade adjuvants. All other authors declare no competing interests. **Data and materials availability:** Sequencing data from the V4 region of the 16S rRNA gene of tumor-associated and fecal bacteria is deposited at the BioProject database (BioProject ID:PRJNA528297; https://www.ncbi.nlm.nih.gov/bioproject/528297).

SUPPLEMENTARY MATERIALS

science.sciencemag.org/cgi/content/full/science.abc3421/DC1
Materials and Methods
Figs. S1 to S22
Tables S1 and S2
References (*48*–*65*)
MDAR Reproducibility Checklist

20 April 2020; resubmitted 7 July 2020
Accepted 30 July 2020
Published online 13 August 2020
10.1126/science.abc3421

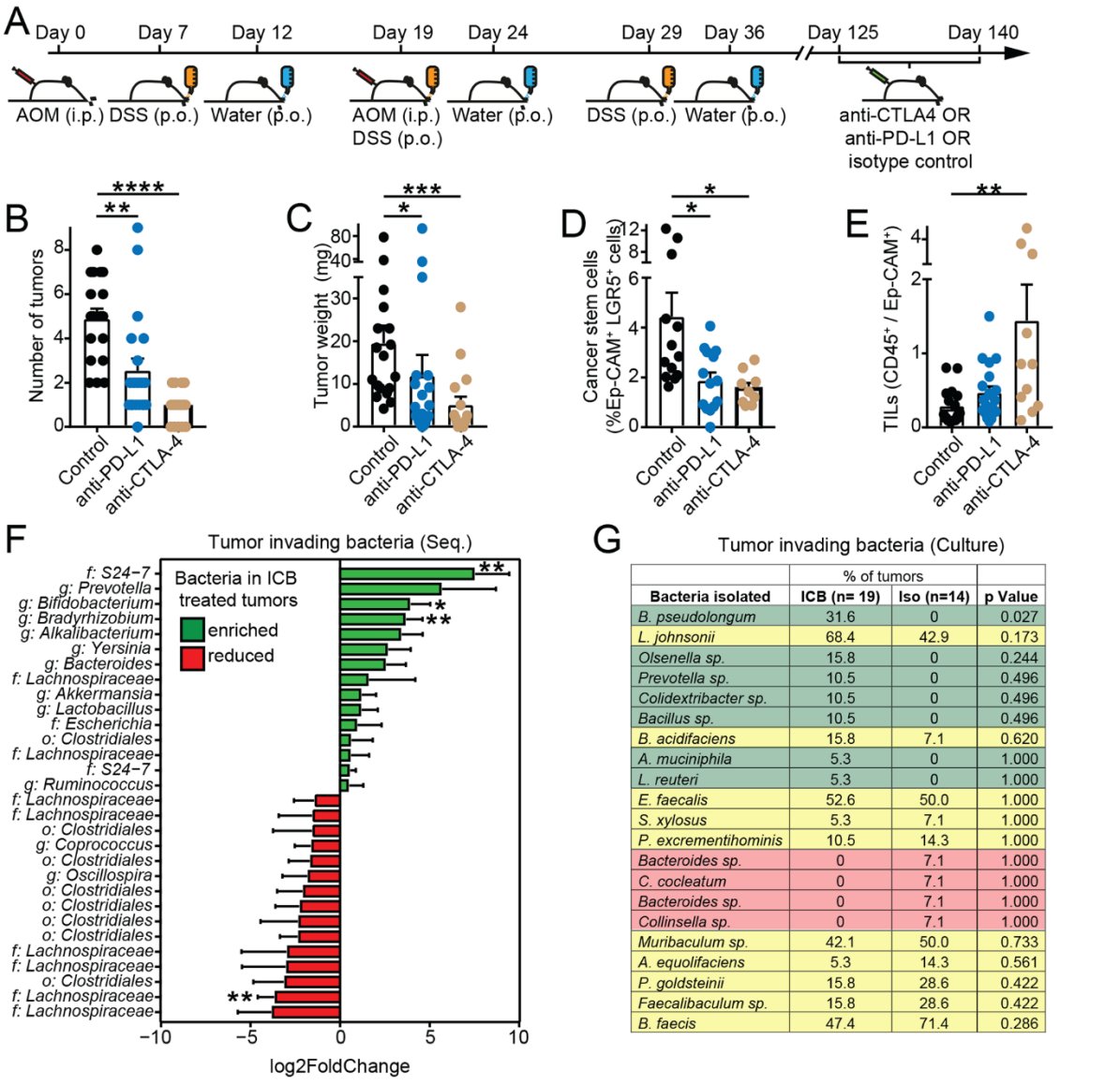

Bacteria isolated	% of tumors ICB (n= 19)	% of tumors Iso (n=14)	p Value
B. pseudolongum	31.6	0	0.027
L. johnsonii	68.4	42.9	0.173
Olsenella sp.	15.8	0	0.244
Prevotella sp.	10.5	0	0.496
Colidextribacter sp.	10.5	0	0.496
Bacillus sp.	10.5	0	0.496
B. acidifaciens	15.8	7.1	0.620
A. muciniphila	5.3	0	1.000
L. reuteri	5.3	0	1.000
E. faecalis	52.6	50.0	1.000
S. xylosus	5.3	7.1	1.000
P. excrementihominis	10.5	14.3	1.000
Bacteroides sp.	0	7.1	1.000
C. cocleatum	0	7.1	1.000
Bacteroides sp.	0	7.1	1.000
Collinsella sp.	0	7.1	1.000
Muribaculum sp.	42.1	50.0	0.733
A. equolifaciens	5.3	14.3	0.561
P. goldsteinii	15.8	28.6	0.422
Faecalibaculum sp.	15.8	28.6	0.422
B. faecis	47.4	71.4	0.286

Fig. 1. Identification of bacteria that promote response to immune checkpoint blockade (ICB) therapy. (**A**) Schematic of the experimental setup. Animals were treated with either anti-CTLA-4, anti-PD-L1 or isotype control antibody. (**B**) Number of tumors, (**C**) tumor weight, (**D**) Ep-CAM$^+$, LGR5$^+$ cancer stem cells, and (**E**) tumor-infiltrating leukocytes (TILs) of AOM/DSS intestinal tumors in SPF mice following treatment with isotype-, anti-PD-L1 or anti-CTLA-4 antibodies. (**F**) 16S rRNA gene V4 region amplicon sequencing to identify bacteria in tumor tissue. Bacteria enriched or reduced in tumors of anti-PD-L1/anti-CTLA-4 (ICB) compared to isotype treated animals are shown in green or red, respectively. (**G**) Bacteria cultured from homogenized tumors under anaerobe conditions from anti-PD-L1/anti-CTLA-4 (ICB groups) or isotype (Iso group) treated animals. Bacteria isolated only from ICB-treated tumors shown in green, bacteria isolated only from isotype-treated tumors shown in orange, bacteria isolated from both ICB and isotype-treated tumors shown in yellow. (**H**) Schematic of the experimental setup. (**I**) Tumor growth, (**J**) tumor weight, and (**K**) quantification of intratumoral IFN-γ^+CD8$^+$ and IFN-γ^+CD4$^+$ T cells are shown in germ-free (GF) or monocolonized (*B. pseudolongum*, *Colidextribacter* species, *Lactobacillus johnsonii*, *Olsenella* species, or *Prevotella* species), MC38 tumor bearing mice. Data indicate mean ± SEM [(B) to (E), and (I) to (K)] or (F) mean ±lfcSE (logfoldchangeStandard Error) and pooled from three individual experiments. [(A) to (E)] n = 16–20 mice/group. [(H) to (K)] n = 8–15 mice/group. *, $P < 0.05$; **, $P < 0.01$; ***, $P < 0.001$; ****, $P < 0.0001$.

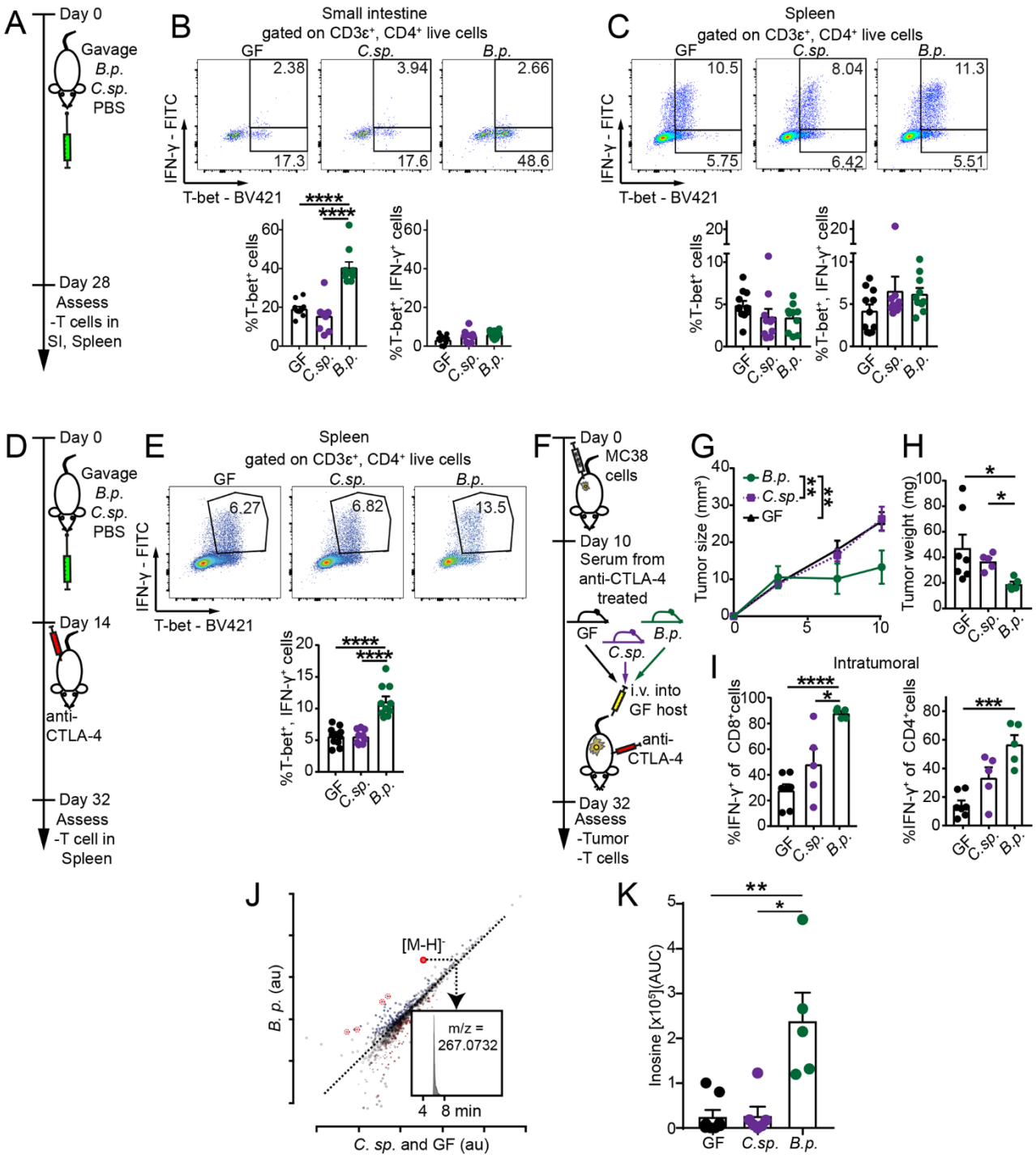

Fig. 2. Effect of *B. pseudolongum* and immune checkpoint blockade on Th1 T cell phenotype and identification of the immunotherapy-promoting metabolite inosine. (**A**, **D**, and **F**) Schematic of the experimental setups. (**B**) representative plots and quantification of T-bet$^+$ and T-bet$^+$IFN-γ^+ events of CD3ε^+CD4$^+$ cells in the small intestine (SI) in the presence of indicated bacteria at day 28. (**C**) same as (B), but in the spleen. (**E**) representative plots and quantification of T-bet$^+$IFN-γ^+ events of CD3ε^+CD4$^+$ T cells in the spleen in the presence of indicated bacteria and anti-CTLA-4 treatment at day 32. (**G**) Tumor growth and (**H**) weight are shown 32 days after MC38 tumor challenge and subsequent serum transfer as well as anti-CTLA-4 treatment. (**I**) quantification of intratumoral IFN-γ^+CD8$^+$ and IFN-γ^+CD4$^+$ T cells. (**J**) Scatter plot of untargeted metabolomics data in the serum of anti-CTLA-4 treated, tumor-bearing *B. pseudolongum* monocolonized compared to *Colidextribacter* species monocolonized and GF mice. Red circles or dotted red circles depict inosine or inosine fragments/adducts, respectively. Inset shows an extracted ion chromatogram of inosine. (**K**) Intensity of inosine (AUC: area under the curve) in sera shown in panel (J) of this figure. Data indicate mean ± SEM and pooled from two individual experiments [(A) to (E)] n = 10–11 mice/group, [(F) to (K)] n = 5–8 mice/group. *, $P < 0.05$; **, $P < 0.01$; ***, $P < 0.001$; ****, $P < 0.0001$.

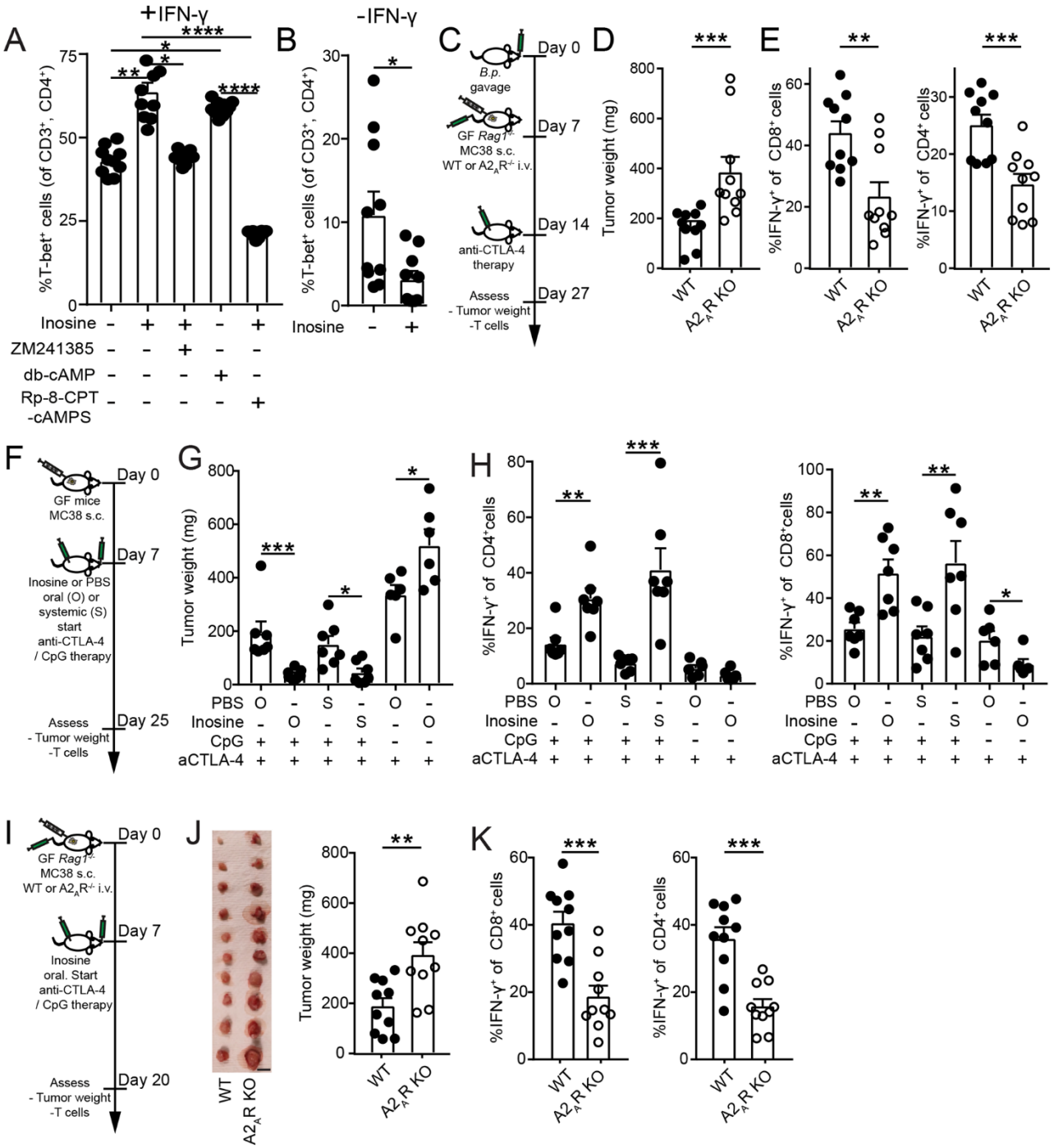

Fig. 3. Inosine promotes Th1 activation and anti-tumor immunity. (**A**) Naïve $CD4^+$ T cells were co-cultured with bone marrow derived dendritic cells and IFN-γ. Quantification of T-bet^+, $CD3^+$, $CD4^+$ T cells 48 hours after co-culture in the presence or absence of inosine, A_{2A} receptor inhibitor (ZM241385), cell permeable cAMP (db-cAMP) and protein kinase A inhibitor (RP-8-CPT-cAMPS). (**B**) Same as (A) without IFN-γ. (**C**) Schematic overview to assess the requirement of $A_{2A}R$ signaling for *B. pseudolongum*-induced anti-tumor immunity. Germ-free (GF) Rag-1-deficient mice were gavaged with *B. pseudolongum* and seven days later 1×10^6 MC38 cells (s.c.) and WT or $A_{2A}R$-deficient 1×10^7 T cells (i.v. 6×10^6 $CD4^+$ and 4×10^6 $CD8^+$ T cells) were injected. Upon palpable tumors, mice were treated with 100µg anti-CTLA-4 (4 times every 72 hours). (**D**) Tumor weight and (**E**) quantification of IFN-γ^+ in $CD8^+$ or $CD4^+$ T cells in the tumor are shown. (**F**) Schematic overview of experimental setup to assess the effect of inosine on anti-tumor immunity. Upon palpable tumors, mice were treated with 100 µg anti-CTLA-4 i.p. (5 times every 72 hours) and in some groups 20 µg CpG i.p. (5 times every 72 hours). In addition, inosine (300 mg/KG/BW) or PBS was given daily orally (O) through gavage or systemically (S) through i.p. injection. (**G**) Tumor weight and quantification of intratumoral IFN-γ^+ cells amongst (**H**) $CD4^+$ or $CD8^+$ T cells are shown. (**I**) Schematic overview to assess the requirement of $A_{2A}R$ signaling for inosine-induced anti-tumor immunity. 1×10^6 MC38 cells (s.c.) and WT or $A_{2A}R$-deficient 1×10^7 T cells (i.v. 6×10^6 $CD4^+$ and 4×10^6 $CD8^+$ T cells) were injected into GF Rag-$1^{-/-}$ mice. Upon palpable tumors, mice were treated with 100 µg anti-CTLA-4, 20 µg CpG (4 times every 72 hours, both i.p.) and inosine (daily, 300 mg/KG/BW, through gavage). (**J**) Pictures of tumors and tumor weight are shown at day 20. Scale bars: 1 cm. (**K**) Quantification of IFN-γ^+ in $CD8^+$ or $CD4^+$ T cells in the tumor are shown. Data indicate mean ± SEM and pooled from two individual experiments [(A) and (B)] n = 10 biological replicates/group and [(C) to (K)] n = 6–10 mice/group. *, $P < 0.05$; **, $P < 0.01$; ***, $P < 0.001$; ****, $P < 0.0001$.

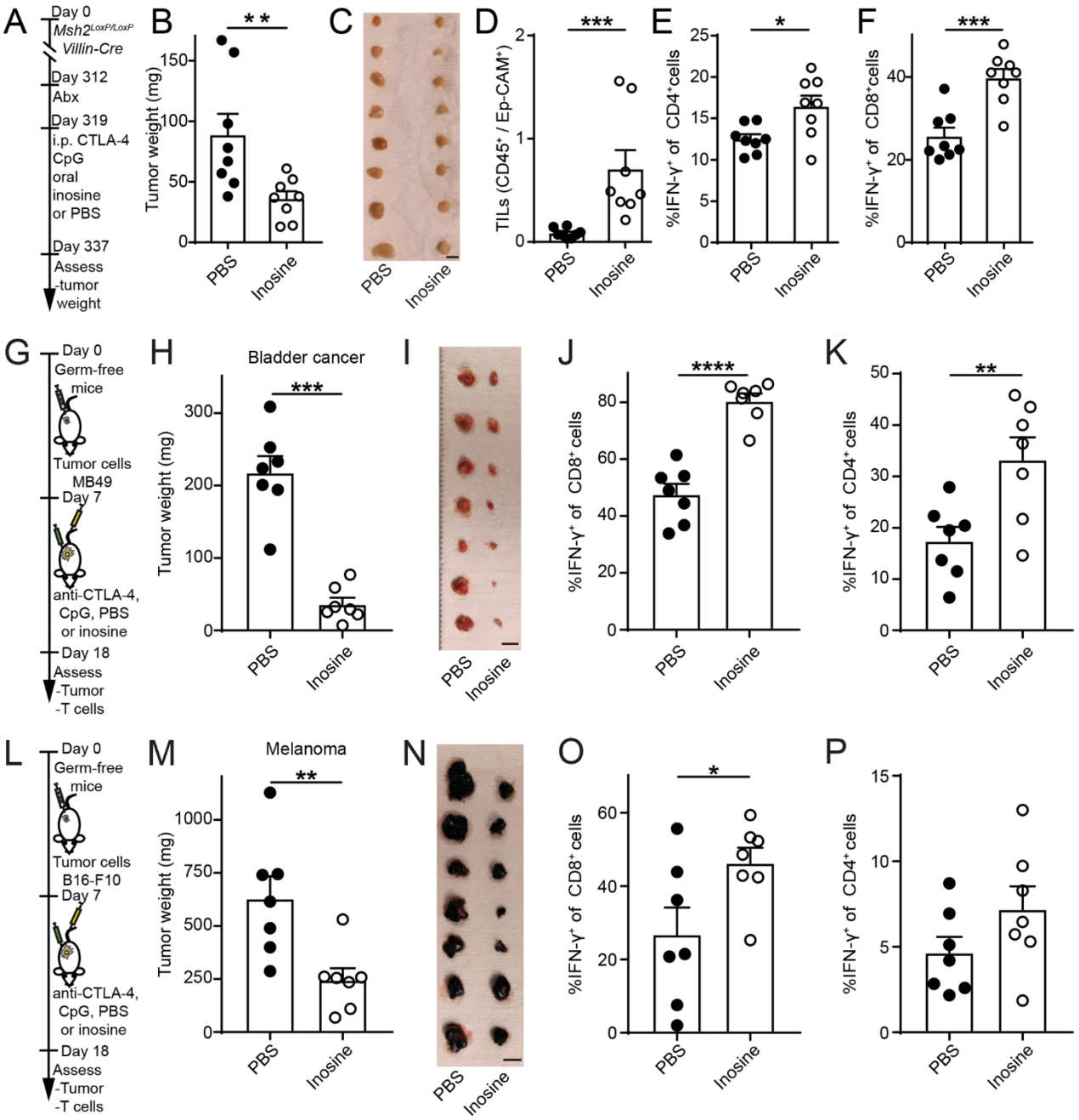

Fig. 4. The metabolite inosine promotes immunotherapy response in mouse models of intestinal cancer, bladder cancer and melanoma. (**A**) Schematic overview of experimental setup to assess the effect of inosine in SPF *Msh2*$^{LoxP/LoxP}$ *Villin-Cre* mice. On day 312, mice received antibiotics orally (Ampicillin 1 mg/ml, Colistin 1 mg/ml and Streptomycin 5 mg/ml) until the end of the experiment and on day 319 mice received 100 µg anti-CTLA-4 i.p., 20 µg CpG i.p. (both 5 times every 72 hours) and PBS or inosine (300 mg/KG/BW) orally through gavage daily. (**B**) Tumor weight, (**C**) representative pictures of dissected tumors (scale bar: 1 cm), (**D**) quantification of tumor-infiltrating leukocytes (TILs) and splenic IFN-γ^+ production of (**E**) CD4$^+$ and (**F**) CD8$^+$ T cells is shown. (**G**) Schematic overview of experimental setup to assess the effect of inosine on bladder cancer. 2×10^6 MB49 bladder cancer cells were injected s.c. in the flank of germ-free animals. Upon palpable tumors, mice were treated with 100 µg anti-CTLA-4 i.p., 20 µg CpG i.p. (3 times every 72 hours) and PBS or inosine (300 mg/KG/BW) orally through gavage daily. (**H**) Tumor weight and (**I**) pictures of tumors are shown. Scale bars: 1 cm. Quantification of IFN-γ^+ in (**J**) CD8$^+$ or (**K**) CD4$^+$ cells in the tumor are shown. (**L**) Schematic overview of experimental setup to assess the effect of inosine on melanoma. 1×10^6 B16-F10 melanoma cells were injected s.c. in the flank of germ-free animals. Upon palpable tumors, mice were treated with 100 µg anti-CTLA-4 i.p., 20 µg CpG i.p. (3 times every 72 hours) and PBS or inosine (300 mg/KG/BW) orally through gavage daily. (**M**) Tumor weight and (**N**) pictures of tumors are shown. Scale bars: 1 cm. Quantification of IFN-γ^+ in (**O**) CD8$^+$ or (**P**) CD4$^+$ cells in the tumor are shown. Data indicate mean ± SEM. [(A) to (F)] n = 8 mice/group. [(G) to (P)] n = 7 mice/group. *, $P < 0.05$; **, $P < 0.01$; ***, $P < 0.001$, ****, $P < 0.0001$.

Microbiome-derived inosine modulates response to checkpoint inhibitor immunotherapy

Lukas F. Mager, Regula Burkhard, Nicola Pett, Noah C. A. Cooke, Kirsty Brown, Hena Ramay, Seungil Paik, John Stagg, Ryan A. Groves, Marco Gallo, Ian A. Lewis, Markus B. Geuking and Kathy D. McCoy

published online August 13, 2020